

# A Distributed Framework for Causal Modeling of Performance Variability in GPU Traces

Ankur Lahiry<sup>[0009-0002-6770-4320]1</sup>, Ayush Pokharel<sup>[0009-0004-1254-9436]1</sup>,  
 Banooqa Banday<sup>[0009-0001-5984-393X]1</sup>, Seth Ockerman<sup>[0000-0002-5692-9359]2</sup>,  
 Amal Gueroudji<sup>[0009-0004-4830-3139]3</sup>, Mohammad Zaeed<sup>[0000-0002-3312-5462]1</sup>,  
 Tanzima Z. Islam<sup>[0000-0003-2877-5871]1</sup>, and Line  
 Pouchard<sup>[0000-0002-2120-6521]4</sup>

<sup>1</sup> Texas State University, San Marcos, TX 78666, USA

{tvty8, ssu22, banooqa, tanzima}@txstate.edu, tz2201@gmail.com

<sup>2</sup> University of Wisconsin-Madison, Madison, WI 53706, USA

sockerman@cs.wisc.edu

<sup>3</sup> Argonne National Laboratory, Lemont, IL 60439, USA

agueroudji@anl.gov

<sup>4</sup> Sandia National Laboratories, Albuquerque, NM 87123, USA

1cpouch@sandia.gov

**Abstract.** Large-scale GPU traces play a critical role in identifying performance bottlenecks within heterogeneous High-Performance Computing (HPC) architectures. However, the sheer volume and complexity of a single trace of data make performance analysis both computationally expensive and time-consuming. To address this challenge, we present an end-to-end parallel performance analysis framework designed to handle multiple large-scale GPU traces efficiently. Our proposed framework partitions and processes trace data concurrently and employs causal graph methods and parallel coordinating chart to expose performance variability and dependencies across execution flows. Experimental results demonstrate a 67% improvement in terms of scalability, highlighting the effectiveness of our pipeline for analyzing multiple traces independently.

**Keywords:** GPU Traces · Performance Variability · Performance Bottlenecks · Causality.

## 1 Introduction

Modern high-performance computing (HPC) systems increasingly integrate heterogeneous architectures combining multi-core CPUs, GPUs, advanced memory hierarchies, and high-speed interconnects. GPUs, in particular, drive most compute-intensive workloads due to their massive parallelism and efficiency in accelerating large-scale simulations and AI models. Yet, this architectural complexity introduces serious optimization challenges. Even small inefficiencies at the kernel or memory level can create performance bottlenecks, leading to severe throughput degradation. Understanding these inefficiencies requires detailed

GPU trace analysis—an indispensable tool for characterizing execution behavior and uncovering root causes of performance loss. However, large-scale GPU traces can reach hundreds of gigabytes per run, making sequential analysis prohibitively slow and resource-intensive. To address this challenge, we develop an end-to-end parallel performance analysis framework for large-scale GPU traces. Our work makes three key contributions:

- Design a scalable distributed framework that parallelizes GPU trace analysis across compute nodes, achieving high throughput and substantially reducing time-to-insight.
- Leverage causal inference-based algorithms that extract variability patterns and link them to system-level inefficiencies, revealing root causes of performance degradation across executions.
- Integrate a complete end-to-end pipeline that automates data ingestion, parallel processing, and insight generation, turning raw GPU telemetry into actionable performance knowledge.

## 2 Methodology

### 2.1 Features

In GPU computing, a kernel is a user-defined function executed in parallel by thousands of threads. Each kernel launch specifies a grid-block configuration that defines how threads are organized and scheduled. During execution, kernels interact with multiple memory hierarchies—registers, shared, global, and cache—each affecting latency and throughput. Although a kernel’s internal logic remains constant across invocations, its performance metrics such as runtime and memory transfer time often fluctuate due to resource contention and hardware variability. Identifying this variability requires analyzing the feature space captured during profiling. GPU profiling tools such as NVIDIA CUPTI [18], Klaraptor [1], and ROCm [13] expose different sets of kernel features. Table 1 summarizes the grouped mapping of these profiler columns to their simplified names used for subsequent causal analysis.

### 2.2 Targets

**Kernel Variability** Let  $K$  be the set of all kernel identifiers in a given performance dataset. For a given kernel  $k \in K$ , which is repeated  $n$  times, we define  $\mathcal{R}_k = \{r_{k,1}, r_{k,2}, \dots, r_{k,n_k}\}$  as the execution of that kernel. We define kernel variability as the extent to which a kernel execution time differs from the **average kernel execution time for each configuration** calculated by  $\bar{r}_k = \frac{1}{n_k} \sum_{i=1}^{n_k} m(r_{k,i})$ . So, the **run-to-run variation** of a given kernel can be calculated by measuring the difference between the execution time of each repeated run and the average kernel execution time for that configuration:  $v_{\text{abs}}(r_{k,i}) = |m(r_{k,i}) - \bar{m}_k|$ .

Table 1: Profiler column names are simplified and grouped into four categories to enhance clarity. The original columns remain in the dataset, but the simplified names improve visualization and interpretation in the causal graphs presented later.

Identification and Context	
Original	Simplified
Kernel_Name, Device, CC, Process_Name, Host_Name	Kernel_Name, Device, CC, Process_Name, Host_Name
Kernel Launch Configuration	
Grid_Size, Workgroup_Size	grid_size, workgroup_size
LDS_Per_Workgroup, Scratch_Per_Workitem	lds_per_workgroup, scratch_per_workitem
[Arch, Accum] VGPR, SGRP, wave_size	[arch, accum]_vgpr, sgrp, wave_size
Temporal Characteristics	
runtime	runtime
SQ_[WAVES, BUSY_CYCLES, CYCLES]	sq_[waves, busy_cycles, cycles]
SQ_INSTS_[VALU, SALU, VMEM]	sq_insts_[valu, salu, vmem]
Memory System Activity	
TCC_[RW_REQ, BUSY, TAG_STALL, HIT, MISS, READ, WRITE]_sum	tcc_[rw_req, busy, tag_stall, hit, miss, read, write]
TCP_PENDING_STALL_CYCLES_sum	tcp_pending_stall
TA_BUFFER_[READ, WRITE]_WAVEFRONTS_sum	ta_buf_[read, write]
TD_[LOAD, STORE]_WAVEFRONT_sum	td_[load, store]

**Memory Stall Variability** GPU kernels often overlap computation and memory operations. However, in many cases, memory operations extend beyond the kernel’s active execution window, creating stalls. To quantify this behavior, we track the start and end times of both the kernel execution and the corresponding memory transfers. For each kernel  $k \in K$ , we observe a set of runs  $\mathcal{R}_k = \{(r_{k,i}^s, r_{k,i}^e) \mid i = 1, \dots, n_k\}$ , where  $r_{k,i}^s$  and  $r_{k,i}^e$  denote the start and end times of the  $i$ -th run of kernel  $k$ , respectively. Similarly, we record the associated memory transfer intervals  $\mathcal{M}_k = \{(m_{k,i}^s, m_{k,i}^e) \mid i = 1, \dots, n_k\}$ , where  $m_{k,i}^s$  and  $m_{k,i}^e$  denote the start and end times of the memory transfer linked to the  $i$ -th run. We compute the absolute difference between kernel duration and the memory transfer interval and define the difference as memory stall variability.

### 2.3 Binning to Reduce Samples

GPU traces record detailed information about every kernel execution over time and often reach massive sizes, making full-trace analysis both memory-intensive and difficult to interpret. To manage this complexity, the trace is divided into fixed-length time segments, called bins, where each bin represents a portion of

the GPU’s execution timeline. All kernel activities that begin within a given bin are grouped together, and a set of summary statistics—such as minimum, maximum, mean, variance, standard deviation, quartiles, and sample count—is computed to describe their behavior. These statistics quantify how stable or variable the performance is within that time window: for instance, variance and standard deviation measure how widely the data values differ, while quartiles help detect unusual outliers. By analyzing the trace one bin at a time, regions showing significant runtime or resource usage fluctuations can be isolated. Bins are then ranked according to their variability, allowing the most critical time periods to be examined in greater depth. This binning approach reduces data size, preserves essential performance trends, and enables independent analysis across different parts of the execution timeline.

## 2.4 Distributed Parallel Architecture

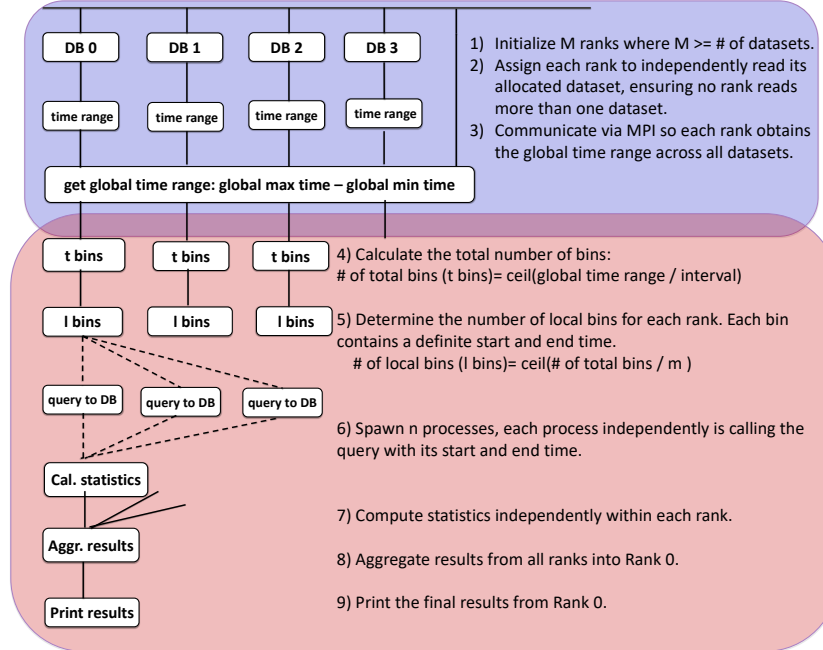


Fig. 1: Overview of the parallel GPU trace analysis framework. The system combines MPI-based distributed parallelism with shared-memory threading to process large GPU activity traces efficiently. MPI ranks divide the workload across nodes (Steps 1–4), each spawning local worker processes to analyze bins in parallel (Steps 5–7). Results are then aggregated (Step 8), and high-variability bins are identified for detailed analysis (Step 9).

Figure 1 shows the overall architecture of our framework. Our system handles large numbers of GPU activity traces in parallel using hybrid MPI and shared-memory parallelism for maximum resource utilization on modern HPC systems.

The program launches multiple MPI ranks, each responsible for a portion of the workload (**Step 1**). The workload consists of bins obtained by segmenting the global execution timeline into fixed-length intervals (**Step 2**). Ranks collaborate to compute the global time range by querying their dataset for minimum and maximum timestamps, then combining values using collective communication (**Step 3**). Each rank is assigned a balanced subset of bins (**Step 4**). After obtaining the end-to-end execution time, we launch worker pools, where each worker processes their assigned bins (**Step 5**). A worker is an independent process created using Python’s multiprocessing module within an MPI rank. Each worker concurrently retrieves its assigned bins from the dataset, performs the analysis, and applies the variability-based filter to retain only the most relevant bins. Low-variability bins are discarded from further analysis, keeping only the top  $K = 5$  highest-variance bins for future computation like identifying the causality, memory stall etc. This hybrid approach achieves two goals: 1) parallel processing of multiple datasets and 2) scalable processing of large datasets.

## 2.5 Causal Modeling

Causal modeling [11] is a systematic approach for discovering and quantifying cause-and-effect relationships within data. Unlike correlational methods, which reveal associations without explaining why they occur, causal modeling enables reasoning about how changes in one variable may directly influence another. This shift from describing patterns to explaining mechanisms allows researchers to move from observation to intervention and prediction. A causal model encodes assumptions about how variables interact and uses these assumptions to estimate directional effects. It is typically represented as a directed graph or a system of equations that specifies which variables act as causes, which as effects, and which serve as confounders—factors that influence both. Once this structure is defined, statistical and computational techniques are applied to estimate causal strengths and to simulate counterfactuals—scenarios that ask, what would happen if a specific change or intervention were made?

## 2.6 Output

**Causal Graph for understanding influence of features on variability**  
 Directed causal graphs reveal how different GPU performance metrics influence one another, distinguishing direct from indirect effects. Unlike correlation plots, they expose which factors most strongly contribute to performance bottlenecks. In our graph, black and red arrows denote positive and negative influences, respectively, with arrow weights indicating each feature’s percentage contribution to performance variance.

**Parallel Coordinate plots for High-Dimensional Trace analysis** Parallel coordinate plots visualize high-dimensional GPU trace data, where each axis represents a performance feature and each line corresponds to a single trace. This view enables simultaneous comparison across metrics, helping identify patterns,

correlations, and clusters of traces that exhibit similar behaviors or performance anomalies.

### 2.7 Performance

We evaluate pipeline performance through a scalability study, assessing its ability to process larger workloads and datasets without a proportional rise in execution time. As shown in Figure 1, the framework achieves near-linear scalability by analyzing multiple GPU trace datasets concurrently when they share common features and target metrics. Each dataset follows an independent processing path with no shared-state contention, ensuring that work on one trace does not delay another. This design enables efficient horizontal scaling across datasets and sustained performance at increasing analysis loads.

## 3 Experimental Setup

Table 2: Comparison of the workflow-level and performance counter datasets, showing their sample and feature sizes, number of kernels, and associated target metric.

Category	Dataset	Samples	Columns	# Kernels	Target Metric
Workflow [9, 3]	Rank 0	~ 837K	28	74	Kernel_variability
	Rank 0	~ 93M	35	74	memory_stall
	Rank 1	~ 837K	28	74	Kernel_variability
	Rank 1	~ 93M	35	74	memory_stall
	Rank 2	~ 837K	28	74	Kernel_variability
	Rank 2	~ 93M	35	74	memory_stall
	Rank 3	~ 837K	28	74	Kernel_variability
	Rank 3	~ 93M	35	74	memory_stall
PerfCounter [16, 6, 12]	Inversek2j-CUDA	1642	8006	1	gpu_time_duration.avg
	Accuracy-CUDA	1200	2119	1	gpu_time_duration.avg
	SW4Lite-CUDA	1201	5036	17	gpu_time_duration.avg

### 3.1 Dataset Description

We categorize seven datasets into two groups, as summarized in Table 2, which lists the number of kernels and target metric for each.

### 3.2 System

Texas Advanced Computing Center (TACC) provides supercomputing facilities to researchers for conducting simulations. We leverage the Lonestar6 computing cluster for running all our experiments. Lonestar6 consists of 560 compute nodes and 88 GPU nodes. Each compute node is comprised of 2 AMD EPYC 7763 64-core (Milan) CPUs and 256 GB of DDR4 memory. Additionally, each of the 84 GPU nodes has 3 NVIDIA A100 GPUs with 40 GB of HBM2 high-bandwidth memory.

## 4 Result

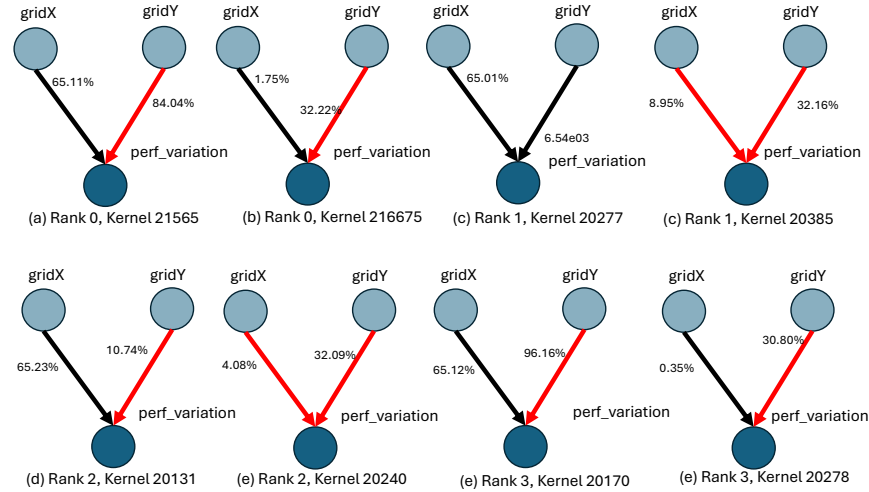


Fig. 2: Kernel variability across different ranks and Kernel. Each row illustrates four examples: (a–d) correspond to Ranks 0–1 and (e–h) to Ranks 2–3. Kernel X refers to the associated `demangledName`, with two kernels randomly selected from different rank datasets. The target is `kernel_duration`, and `perf_variation` is computed as  $|\text{avg}(\text{kernel\_duration}) - \text{kernel\_duration}|$ . Black arrows indicate positive influence (e.g., increasing `gridX` increases variability), while red arrows indicate negative influence on `perf_variablity`. Edge weight defines change of % of a feature has positive or negative influence on `perf_variation`

### 4.1 Kernel Variability

**Workflow Datasets (Per-Kernel) :** In Figure 2, we show kernel variability across rank datasets, where each sub-figure presents a causal graph for a per-kernel group defined by its `demangledName`. `perf_variability` is computed as  $|\text{avg}(\text{kernel\_duration}) - \text{kernel\_duration}|$ . Black arrows denote positive influence, while red arrows denote negative influence on `perf_variablity`. In Figures 2a and 2b, feature `gridX` shows a positive effect and `gridY` a negative effect, though with differing magnitudes—likely due to architectural or workload factors such as memory access or thread parallelism. For the Rank 1 dataset (in Figure 2c and 2d), however, the dominance diagram flips, with the same features exerting opposite influences depending on kernel behavior. Similar shifts appear in Rank 2 and Rank 3 kernels. Overall, these examples illustrate that across all ranks, both the sign and strength of feature-performance relationships vary, showing that kernel-level performance is shaped by rank- and kernel-specific causal dynamics rather than a uniform pattern.

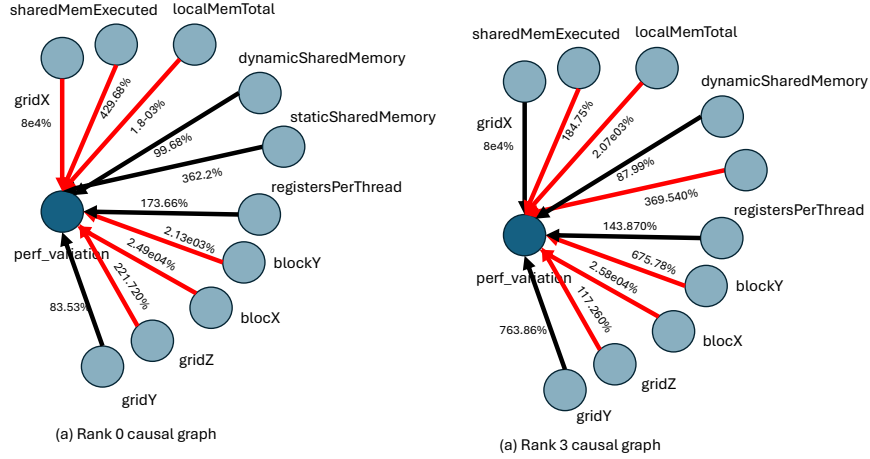


Fig. 3: Overview of kernel variability across ranks and kernels. This figure combines results from all kernels to illustrate variability across different ranks. Due to space constraints, only two representative kernels are randomly selected and shown. The target is `kernel_duration`, and `perf_variation` is computed as  $|\text{avg}(\text{kernel\_duration}) - \text{kernel\_duration}|$ . Edge weight defines change of % of a feature has positive or negative influence on `perf_variation`.

**Workflow Datasets(Entire Dataset)** : In Figure 3, we extend the analysis with Rank 0 and Rank 3 kernel groups by combining all of the kernel groups. In the Rank 0 causal graph (Fig. 3a), kernel-features such as `gridY` and Memory-related features such as `dynamicSharedMemory`, `staticSharedMemory`, and `registersPerThread` contribute positively, whereas `gridX`, `blockX`, and `blockY` exert weaker negative effects. We also see the same feature influence in the Rank 3 causal graph (Fig. 3b).

#### 4.2 Parallel Coordinate of Memory Stall Variability

**Impact of Grid Size on Kernel Variability** : The analysis in Figure 4 reveals that a high `gridX` value is strongly associated with increased kernel variability. Larger grid dimensions imply the launch of a greater number of thread blocks, which, in turn, elevates the complexity of scheduling and load balancing on the GPU. This heightened complexity can introduce fluctuations in execution times across different invocations of the same kernel. Consequently, rather than stabilizing performance, scaling the grid in this way appears to amplify performance dispersion, underscoring the sensitivity of kernel behavior to launch configuration parameters.

**Influence of Copy Kind on Kernel Variability** : Memory transfer characteristics also show a substantial effect on kernel variability. From Figure 4, we observe operations with `copyKind = 8` (*Device-To-Device*) exhibit pronounced instability compared to other transfer modes. This copy kind likely corresponds

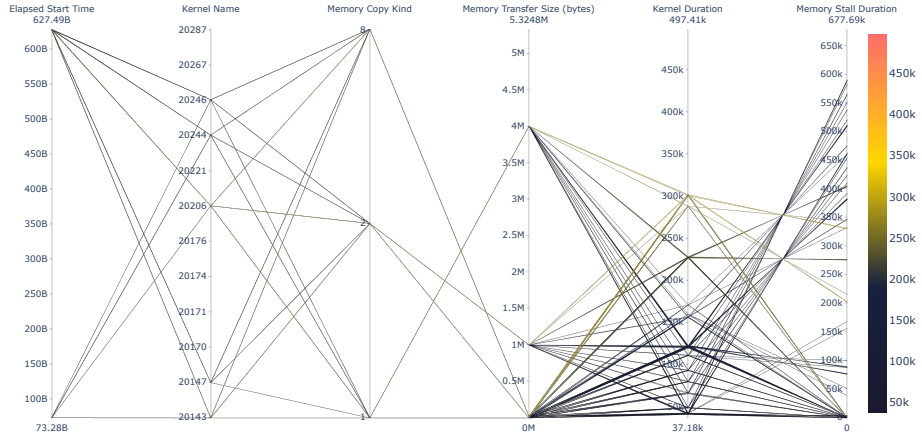


Fig. 4: Parallel coordinates plot illustrating kernel execution characteristics under varying memory access scenarios for the Rank 3 dataset. Each line represents an individual kernel invocation, with axes corresponding to elapsed start time, kernel name, memory copy kind, memory transfer size, kernel duration, and memory stall duration. Line colors encode kernel duration, revealing correlations between transfer size and stall time that highlight performance bottlenecks in memory-bound operations.

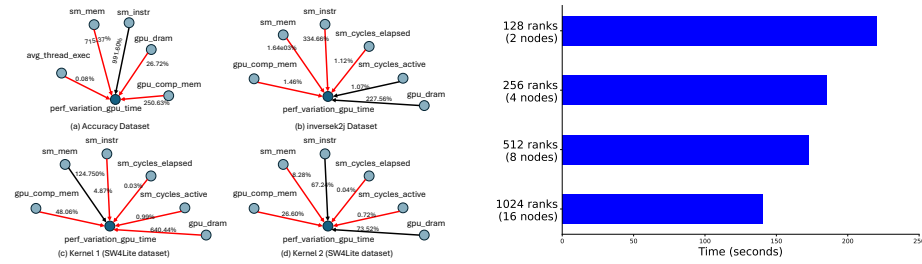
to a transfer type or direction that imposes additional overhead—such as involving nonstandard paths, asynchronous transfers, or higher latency variability. These irregularities in transfer behavior contribute to inconsistent overlaps with kernel execution, which is reflected in elevated variability metrics.

### 4.3 PerfCounter Dataset

Figure 5a illustrates the causal relationships within the **PerfCounter** datasets. All three datasets exhibit identical feature characteristics, and `gpu_time` serves as the performance metric, represented as `perf_variation_gpu_time`. Kernels are categorized by `KERNEL_NAME`. Consequently, per-kernel and overall causality assessments coincide for `inversek2j-CUDA` and `Accuracy-CUDA`. Across all cases, memory-related factors (`sm_mem`, `gpu_dram`) and instruction metrics (`sm_instr`) consistently exhibit a dominant influence on performance variability. In the `Accuracy` dataset (a), `gpu_comp_mem` and `avg_thread_exec` emerge as significant contributors; whereas, in `inversek2j` (b), `sm_cycles` assumes greater importance. For Kernels 1 and 2, similar causal drivers reappear with differing magnitudes, underscoring workload-dependent causal patterns and stable directional influences with variable intensities across datasets.

## 5 Scalability

We run memory stall experiments in parallel, consisting of 10.38 minutes of memory traces per workflow dataset. Each dataset contains approximately 93



(a) Kernel variability in **PerfCounter**: black = positive, red = negative influence. (b) For fixed input, execution time decreases as MPI ranks increase.

Fig. 5: Overview of variability and scalability, illustrating performance behavior across datasets and ranks.

million samples (Table 2), and we process four datasets concurrently. With a 10 ms interval, each yields about 68.8K bins, totaling roughly 272.2K bins. From Figure 5b, for a fixed input size, the pipeline shows clear scalability as MPI ranks increase: execution time drops from 240s at 128 ranks to 180s at 256 (25%), 120s at 512 (50%), and 80s at 1024 (67%), confirming efficient workload distribution and steady runtime reduction with growing concurrency. However, perfect linear speedup is constrained by non-parallelizable setup operations (e.g., input reading, global time range computation, bin partitioning) and by communication overheads, load imbalance, I/O contention, and Rank 0 aggregation, which collectively impose a scaling floor.

## 6 Related Work

Modern GPU architectures have become increasingly complex to meet growing demands in scientific computing, AI, and data-driven applications, requiring efficient resource utilization. Heterogeneous systems now feature specialized cores, deeper memory hierarchies, and complex scheduling, making performance bottleneck analysis critical. Yang et al. [15] extended the Empirical Roofline Toolkit to NVIDIA FP64/FP32/FP16 and Tensor Cores, collecting kernel time, FLOPs, and memory traffic with Nsight Compute. Validated on DeepCAM (TensorFlow and PyTorch), their hierarchical Roofline analysis revealed Tensor Core utilization, cache locality, AMP effects, and zero-AI kernel overhead, distinguishing compute- vs. bandwidth-bound behavior. Elvinger et al. [2] profiled fine-grained resource interference (.schedulers, IPC/warp, pipelines, caches, memory) on H100 and RTX 3090 using microbenchmarks, exposing metric limits and motivating interference-aware scheduling. For AMD GPUs, Leinhauser et al. [8] introduced an Instruction Roofline Model using ROCProfiler and BabelStream to enable analysis despite missing counters. They derived IRM equations, built instruction-per-byte and wavefront-normalized GIPS rooflines, and applied them to PICo-GPU kernels on V100, MI60, and MI100 for cross-architecture comparison.

In terms of performance modeling in HPC, researchers have also been proposed different idea to find out why performance variability occurs. Wander [7]

introduces a comparable technique for causality analysis in the performance domain. However, their study does not provide evidence regarding the method's scalability or its applicability to large-scale datasets such as ours. Patki et al. [10] quantify performance variability through repeated runs and CoV, focusing on the extent of fluctuations. PADDLE [14] is a unified machine learning framework designed to automate and enhance performance analysis in high-performance computing systems by efficiently handling large-scale performance data and making machine learning more accessible to HPC analysts. Several visualization tools have been introduced in previous studies [4], [5] to effectively illustrate and analyze performance variations in visual data. Though they are visualizing the performance variation, they are still unable to explain the reason "why", which we tried to explain using causality. Opal [17] feeds compact, structured performance insights into a template prompt so that an LLM can generate code edits that explicitly tie each change to the observed runtime bottleneck, along with a rationale and deferred suggestions for unsafe edits. However, Our study identifies the causal drivers of performance variance within a given dataset and quantifies their impact, without proposing code-level changes.

## 7 Conclusion

This paper presents a distributed causal graph framework to explain run-to-run variability in GPU execution time. Micro-level fluctuations in kernel behavior often accumulate, leading to significant variability in end-to-end workflow performance. Understanding these fine-grained variations lays the foundation for future hierarchical analyses that attribute the root causes of workflow-level variability.

## 8 Acknowledgment

This material is based upon work supported by the U.S. Department of Energy, Office of Science under Award Number DE-SC0023173. This material is based upon work supported by the U.S. Department of Energy (DOE), Office of Science, Office of Advanced Scientific Computing Research, under Contracts DE-AC02-06CH11357.

## References

1. Brandt, A., Mohajerani, D., Maza, M.M., Paudel, J., Wang, L.: Klaraptor: A tool for dynamically finding optimal kernel launch parameters targeting cuda programs. arXiv preprint arXiv:1911.02373 (2019)
2. Elvinger, P., Strati, F., Jerger, N.E., Klimovic, A.: Measuring gpu utilization one level deeper. arXiv preprint arXiv:2501.16909 (2025)
3. Gueroudji, A., Phelps, C., Islam, T.Z., Carns, P., Snyder, S., Dorier, M., Ross, R.B., Pouchard, L.C.: Performance characterization and provenance of distributed task-based workflows on hpc platforms. In: SC24-W: Workshops of the International Conference for High Performance Computing, Networking, Storage and Analysis. pp. 2032–2039 (2024). <https://doi.org/10.1109/SCW63240.2024.00254>

4. Islam, T., Ayala, A., Jensen, Q., Ibrahim, K.: Toward a programmable analysis and visualization framework for interactive performance analytics. In: 2019 IEEE/ACM International Workshop on Programming and Performance Visualization Tools (ProTools). pp. 70–77. IEEE (2019)
5. Islam, T.Z., Thiagarajan, J.J., Bhatele, A., Schulz, M., Gamblin, T.: A machine learning framework for performance coverage analysis of proxy applications. In: SC'16: Proceedings of the International Conference for High Performance Computing, Networking, Storage and Analysis. pp. 538–549. IEEE (2016)
6. Jin, Z., Vetter, J.S.: A benchmark suite for improving performance portability of the sycl programming model. In: 2023 IEEE International Symposium on Performance Analysis of Systems and Software (ISPASS). pp. 325–327 (2023). <https://doi.org/10.1109/ISPASS57527.2023.00041>
7. Lahiry, A., Banday, B., Islam, T.Z.: Wander: An explainable decision-support framework for hpc (2025), <https://arxiv.org/abs/2506.04049>
8. Leinhauser, M., Widera, R., Bastrakov, S., Debus, A., Bussmann, M., Chandrasekaran, S.: Metrics and design of an instruction roofline model for amd gpus. ACM Transactions on Parallel Computing **9**(1), 1–14 (2022)
9. Ockerman, S., Gueroudji, A., Mallick, T., He, Y., Pouchard, L., Ross, R., Venkataraman, S.: Pgt-i: Scaling spatiotemporal gnns with memory-efficient distributed training (2025), <https://arxiv.org/abs/2507.11683>
10. Patki, T., Thiagarajan, J.J., Ayala, A., Islam, T.Z.: Performance optimality or reproducibility: that is the question. In: International Conference for High Performance Computing, Networking, Storage and Analysis. pp. 1–30 (2019)
11. Pearl, J.: Causality: Models, Reasoning and Inference. Cambridge University Press, USA, 2nd edn. (2009)
12. Petersson, N.A., Sjogreen, B., Tang, H., Pankajakshan, R.: geodynamics/sw4: SW4, version 3.0 (Sep 2023). <https://doi.org/10.5281/zenodo.8322590>, <https://doi.org/10.5281/zenodo.8322590>
13. Shafie Khorassani, K., Hashmi, J., Chu, C.H., Chen, C.C., Subramoni, H., Panda, D.K.: Designing a rocm-aware mpi library for amd gpus: early experiences. In: International Conference on High Performance Computing. pp. 118–136. Springer (2021)
14. Thiagarajan, J.J., Anirudh, R., Kailkhura, B., Jain, N., Islam, T., Bhatele, A., Yeom, J., Gamblin, T.: Paddle: Performance analysis using a data-driven learning environment. In: 2018 IEEE International Parallel and Distributed Processing Symposium (IPDPS). pp. 784–793 (May 2018). <https://doi.org/10.1109/IPDPS.2018.00088>
15. Yang, C., Wang, Y., Kurth, T., Farrell, S., Williams, S.: Hierarchical roofline performance analysis for deep learning applications. In: Intelligent Computing: Proceedings of the 2021 Computing Conference, Volume 2. pp. 473–491. Springer (2021)
16. Yazdanbakhsh, A., Mahajan, D., Lotfi-Kamran, P., Esmaeilzadeh, H.: AXBENCH: A multi-platform benchmark suite for approximate computing. IEEE Design & Test (2016), special issue on Computing in the Dark Silicon Era
17. Zaeed, M., Islam, T.Z., Indić, V.: Opal: A modular framework for optimizing performance using analytics and llms (2025), <https://arxiv.org/abs/2510.00932>
18. Zhen, Z., Jidong, Z., Yan, L., Wenguang, C.: Workload analysis for typical gpu programs using cupti interface. Journal of Computer Research and Development **53**(6), 1249–1262 (2016). <https://doi.org/10.7544/issn1000-1239.2016.20148354>, <https://crad.ict.ac.cn/en/article/doi/10.7544/issn1000-1239.2016.20148354>